Tectonophysics 712-713 (2017) 723–728

Contents lists available at ScienceDirect

Tectonophysics

journal homepage: www.elsevier.com/locate/tecto

Time-series analysis of earthquake sequences by means of information recognizer

E.E. Vogel[a,b], G. Saravia[a], D. Pastén[c,d], V. Muñoz[c,*]

[a] Departamento de Física, Universidad de La Frontera, Casilla 54-D, Temuco, Chile
[b] Center for the Development of Nanoscience and Nanotechnology (CEDENNA), Santiago 9170124, Chile
[c] Departamento de Física, Facultad de Ciencias, Universidad de Chile, Santiago, Chile
[d] Advanced Mining Technology Center (AMTC), Santiago, Chile

ARTICLE INFO

Article history:
Received 31 January 2017
Received in revised form 20 June 2017
Accepted 26 June 2017
Available online 1 July 2017

JEL classification:
91.30.Px
89.70.-a
89.75.-k

Keywords:
Earthquakes
Information theory
Time series analysis

ABSTRACT

Three seismic sequences of several thousand earthquakes each are analyzed by means of a tunable information recognizer known as wlzip. These sequences are different both in the geographical coverage and the time span, including earthquakes of magnitude larger than 8.0. The main variable under scrutiny here is the time interval between consecutive events. Two parameters (mutability and interval dilation) are defined for each sequence, which relate to the information contained in it. In this way it is possible to characterize different regimes in the seismic activity. For instance, mutability increases before large earthquakes and decreases sharply immediately after each of these events. On the other hand, interval dilation reaches a clear maximum several months before major earthquakes, while it decreases to its lowest possible value after such earthquakes during the aftershock regime. Extensions of the application of this new method to other problems in seismicity are mentioned.

1. Introduction

Tools from the study of complex systems have been useful in the analysis of seismicity (Abe et al., 2011, 2010; Baiesi and Paczuski, 2004; Pastén and Comte, 2014; Pastén et al., 2011; Pastén et al., 2016; Telesca and Lovallo, 2012). Features such as self-similarity, self-organization, patterns, finite-scaling, spatial distribution, and scale-free characteristics have been studied in this context. In particular, various ways to study the time sequence of earthquakes have been investigated (*e.g.* Romashkova, 2009, Telesca et al., 2001, Telesca and Lapenna, 2006, Telesca and Lovallo, 2009, Telesca et al., 2007, Xu and Burton, 2006). On the other hand, seismic hazard is an interesting and important topic of study, which has been dealt with in various ways (Fu et al., 2004; Rotondi and Varini, 2006). New tools can contribute significantly to the understanding of earthquake dynamics, and the purpose of this paper is to suggest an information theory approach to the study of seismicity.

In this sense, one approach has been to focus on the time interval between earthquakes (Abe and Suzuki, 2005; Sarlis et al., 2010; Carlson and Res, 1991; Sarlis et al., 2009; Sarlis and Christopoulos, 2012; Varotsos et al., 2002, 2005). Various features have been studied, such as the statistical properties of the "calm periods", where a scale-free time distribution can be found (Abe and Suzuki, 2005), or the time interval between major events, either for models of seismicity (Carlson and Res, 1991) or for seismic catalogs (Sarlis et al., 2010; Sarlis et al., 2009; Sarlis and Christopoulos, 2012; Varotsos et al., 2005Sarlis et al.). One of the most studied methods to analyze complex time series, and seismic time series in particular, is "natural time". This method involves a reparametrization of time, and can be applied to a number of complex time series arising in various physical and geophysical systems (Abe et al., 2005; Varotsos et al., 2006a; Sarlis and Christopoulos, 2012; Varotsos et al., 2011). For earthquakes, this method has been applied to precursor seismic electric signals by the definition of a *natural time* for the occurrence of the kth event in the time series, namely $\chi_k = k/N$, where N is the number of data. The method of natural time considers the time evolution of the pair (χ_k, E_k), where E_k is the energy released during that event, and it has been shown that the variance of χ for the seismic electrical signals decreases when a mainshock is about to occur

* Corresponding author.
E-mail address: vmunoz@fisica.ciencias.uchile.cl (V. Muñoz).

http://dx.doi.org/10.1016/j.tecto.2017.06.031
0040-1951/

(Varotsos et al., 2006b; Varotsos et al., 2002, 2005). We propose in this paper a different way to analyze the time interval between two seismic events, by using information theory.

Very recently a data analysis method based on information recognition in any time series has yielded useful results on magnetic phase transitions (Vogel et al., 2009, 2012), agitation in stock markets (Vogel and Saravia, 2014), variations in capitalizations towards pensions (Vogel et al., 2015), blood pressure (Contreras et al., 2016), and wind energy (Vogel et al., 2016). In the present paper we apply this powerful technique to the recognition of information of seismological activity. Our results suggest that an indicator can be defined, which begins to increase several months prior to important earthquakes.

The following are the main novel features considered in the present paper. Seismic data from geographical regions around the epicenter of important earthquakes are considered on extended time bases, both before and after these earthquakes. The method based on information theory is invoked to calculate the mutability (a way of variability defined below) of the time series associated to the time interval between consecutive quakes over a predetermined magnitude in the Richter scale. Based on this, an indicator called *interval dilation* or simply *dilation* is constructed. Dilation maximizes over a critical value several months before earthquakes of magnitude about 7.0 or higher. No false overshoots for dilation have been found for periods of lower seismic intensity. Since the behavior is the same for three different geographical areas in different periods of time, we believe this methodology establishes a new way to detect areas where seismic energy can be accumulating.

2. Methodology

2.1. Data organization

We have chosen three large earthquakes occurred in Chile in the last seven years in order to apply this method to seismic data sets that have the same tectonic source, the displacement of Nazca plate (Lonsdale, 2005; Maksymowicz, 2015) under the South American plate (Manea et al., 2017). They correspond to the three following geographical areas of Chile: Central Zone, Iquique and Maule as presented below, and illustrated in Fig. 1. The seismic data set for Iquique had precursory activity, while the seismic data sets for Maule and Central Zone did not. All of them were registered using local measurements, having a high quality (Servicio Sismológico Nacional, 2016).

Major events are collected in Table 1. Each event is assigned a code for future reference. Then the table shows the abscissa (position of each event in the time series): the first seism of the sequence has abscissa 1, and so on. The following columns define the date, and the last column gives the corresponding magnitude.

2.1.1. Central Zone

Seismic events of magnitude 3.0 and higher with hypocenter within 29° and 35.5° South Latitude and between 69° and 74° West Longitude. This series starts on 2 October 2000 and ends on 26 October 2015; it includes the M_w8.3 earthquake near Illapel. Data were obtained through the National Seismological Center (Servicio Sismológico Nacional, 2016). There are 22 693 seismic events in this series. The most important seismic activity for the present analysis (as detailed later in Fig. 2) is listed as C1 through C6 in Table 1. Codes C2 and C4 correspond to several individual events each, very close in time.

2.1.2. Iquique

This data set consists of 8 601 seismic events measured by the National Seismological Center (Servicio Sismológico Nacional, 2016), between 1 January 2012 and 31 August 2015 between 18° and 22° South Latitude and between 68° and 72° West Longitude. It includes the M_w8.2 earthquake occurred near Iquique in 2014. The most important seismic activity for the present analysis (detailed later in Fig. 5) is listed as I1 through I4 in Table 1.

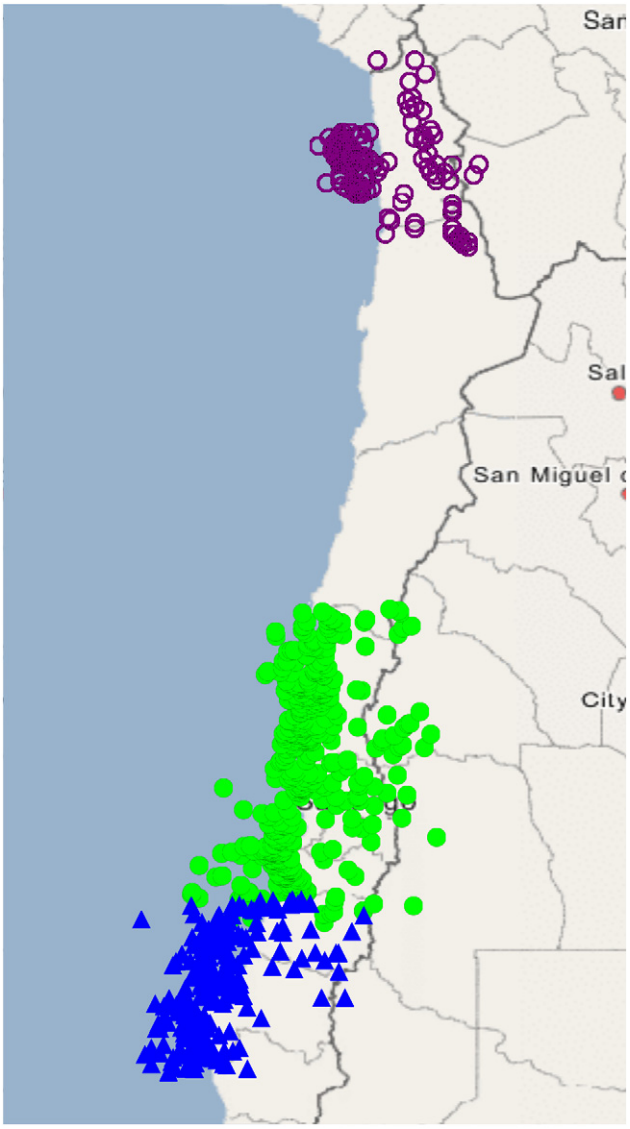

Fig. 1. Epicenter location for the three zones studied. Purple open circles: Iquique; green dots: Central Zone; blue triangles: Maule. For clarity, only data with magnitudes above 5 are shown.

2.1.3. Maule

These data were obtained from the USGS (United States Geological Survey, 2016). It includes 1 253 seisms of magnitude over 4.7 occurred between 33° and 38.5° South Latitude and 71° and 74° West Longitude between 17 January 1973, and 4 July 2012. It includes the M_w8.8 earthquake offshore Bio-Bio and also a M_w7.8 earthquake which is related to a larger previous one M_w8.0 offshore Valparaiso on March 3, 1985. The most important seismic activity for the present analysis (detailed in Fig. 7) is listed as M1 through M4 in Table 1. As it can be noticed in Fig. 1, there is an overlap between Central Zone and Maule regions, so important earthquakes in one of these regions can also produce aftershocks in the neighboring region.

Table 1
Main seisms and characteristics for the three series defined in the text.

	Sequence	Date			Magnitude
Code	Abscissa	Y	M	D	Richter
Central Zone series 3.0+					
C1	621	2001	04	09	6.4
C2	4927–5155	2003	02	02–20	5.5–5.7
C3	7580	2004	08	28	6.2
C4	12,701–12,740	2008	12	18–20	5.1–5.8
C5	13,556	2010	02	27	6.9
C6	21,150	2015	09	16	8.4
Iquique series 3.0+					
I1	382	2012	05	14	6.4
I2	2266	2014	03	16	6.7
I3	2646	2014	04	01	8.2
I4	2819	2014	04	03	7.6
Maule series 4.7+					
M1	119	1985	03	03	7.8
M2	411	2010	02	27	8.8
M3	1120	2011	01	02	7.2
M4	1244	2012	03	25	7.1

The analysis was done on the complete seismic data sets, which for the Central Zone and Iquique correspond to events with magnitude larger than $M_w = 3.0$, and for Maule to events with magnitude larger than $M_w = 4.7$.

2.2. Information recognizer

Data recognizer wlzip (Vogel et al., 2012) was created to recognize repeated meaningful information in any sequence of data. It is freely available upon request (Vogel et al., 2012). Algorithms are similar to those of data compressors which recognize any repeated information regardless of its meaning. However, "word length zipper" (wlzip) recognizes only exact matches of a sequence at specific positions in the numeric information. Thus, compressions done by wlzip represent specific properties of the system. Actually, wlzip compacts less than other compressors like rar or bzip2.

A high degree of compression by wlzip means that repetitive information is present in the data chain; this is characteristic of a system whose properties do not change significantly within the data window under consideration. On the other hand, a very low degree of compression means that repetitive information is scarce in the data chain, namely a system whose properties change constantly along the data chain.

The sequence to be analyzed corresponds to the intervals in minutes between consecutive seisms of magnitude M and larger ($M+$). The dynamical data window over which the information recognition will be conducted comprises a given instant (seism) i and the $\nu - 1$ previous quakes. This portion of the sequence is compressed yielding a weight (in bytes) that will be denoted by $w^*(i,\nu)$.

In order to define *mutability* μ as an indicator with values around 1.0 we define a chain of ν random numbers with as many digits as the maximum number of digits present in the sequence under study. This fixed chain is compressed and its weight is denoted by $W(\nu)$. Then the relative mutability $\mu(i,\nu)$ is simply given by the ratio

$$\mu(i,\nu) = \frac{w^*(i,\nu)}{W(\nu)} \ . \tag{1}$$

In the present work we will consider $\nu = 24$ which gives good contrast for $\mu(i,\nu)$ for the series to be characterized below (one series is also studied for $\nu = 96$, for comparison and to justify our choice; see next section). Larger ν values give smoother results for $\mu(i,\nu)$ but the anticipation feature discussed in the next section is progressively lost. Shorter ν values yield progressively unstable results. Eventually ν can be optimized for each series of data (representing different dynamics) but this is beyond the scope of this paper.

3. Results and discussion

The seismic data for Central Chile provides a 15-year period to test any possible indicator. Fig. 2 gives the results for mutability. The first striking feature are the downward "needles" that happen only occasionally. They are directly linked to major seismic activity which is identified by events C1 through C6 in Table 1; the corresponding labels are placed on scale just over the abscissa axis in Fig. 2.

Another interesting feature is that the deep downward needles, associated to major earthquakes, are followed by periods of low values of μ, changing to an oscillatory recovery along a ramp which lasts several hundreds events (several months). Then, eventually mutability goes back to values close to the range 1.1 or 1.2, which seems to be characteristic for calmed periods in this geographical region. (See for instance the interval going from events 17 000 to 21 000 approximately, which corresponds to almost five years from the end of 2010 to the middle of 2015, just in between the two major earthquakes C5 and C6.)

Why does μ decrease so abruptly for major earthquakes? Immediately after a major earthquake a large amount of aftershocks happen at very short intervals. This means similar intervals in the sequence which wlzip recognizes as such, leading to a high degree of compression, hence low values of mutability. If we were interested in aftershock behavior, wlzip can be tuned to optimize recognition of small numbers, namely, short intervals. However, we want to turn our attention now to the behavior prior to large earthquakes for which the plate subduction off shore in Chile is a natural laboratory.

Fig. 2 also shows that values of $\mu(i,24)$ saturate just before large earthquakes, therefore its usefulness as a sensitive parameter before them is low. However, since calculation of $\mu(i,24)$ is based on detection of repeated sequences of numbers, this lack of sensitivity can be remedied if we improve the performance of wlzip by tuning the digits to be recognized. This is better done on a numerical basis which requires more positions than the usual decimal one to express the same information: we choose here to recognize information in quaternary basis, namely with four digits (0, 1, 2, and 3). Some points

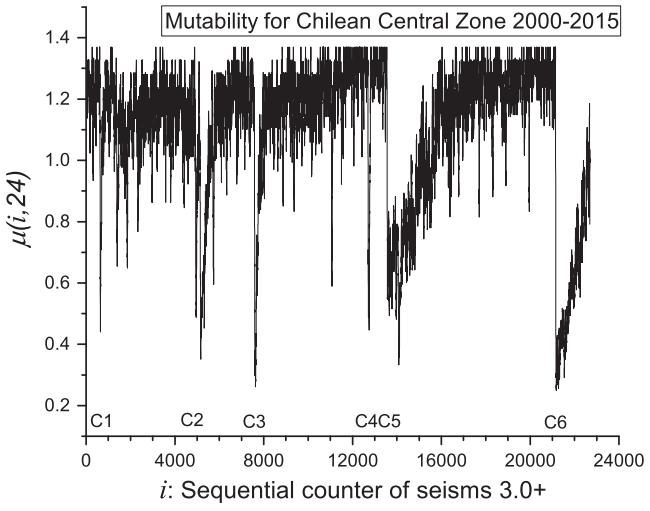

Fig. 2. Mutability for a sequence of 22 693 seisms of magnitude 3.0 and larger for the Central Chile area during about 15 years in the period 2000–2015. Different regimes are recognized and discussed in the text. The signature of the two major earthquakes during this period is clearly recognized.

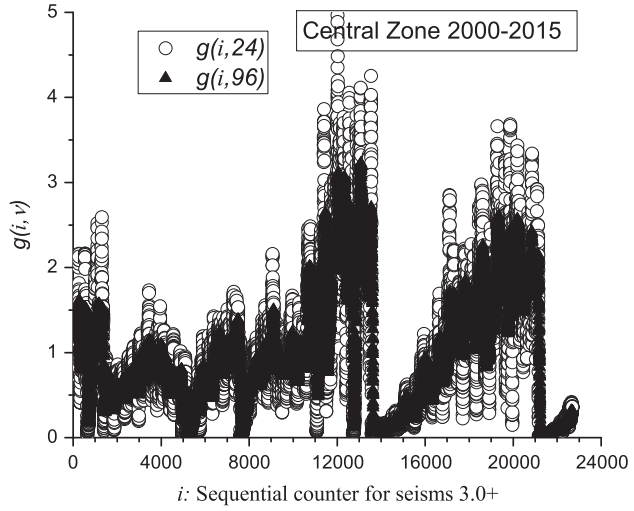

Fig. 3. Amplifying function $g(i,\nu)$ for all the seisms of Central Zone. The average period for ν intervals is previously determined over the full interval ($\langle interval \rangle_{full}$); also, the dynamic average over the last ν events until the i-th one is measured: $\langle interval(i) \rangle_{\nu}$; the ratio of the latter over the former defines $g(i,\nu)$ according to Eq. (3).

in the analyzed sequence of intervals are shown in Table 2, in both decimal and quaternary bases.

After an optimization process (only the interval of 24 instants is justified below, the rest of the optimization is omitted due to space reasons) we settled for recognition of the three positions after the fourth one (digits in positions 4, 5 and 6) in quaternary basis. They are highlighted in boldface in Table 2. It is clear that all short intervals are the same under this precision, thus maximum compression is achieved. On the contrary only two segments of three digits repeat within the long intervals in Table 2 so compression is low and mutability is high.

The mutability obtained in this way is denoted by $\mu(i,24)b4\_4,3$. Here, "*b4*" represents the use of basis 4 to represent all numbers, and "4,3" the fact that 3 relevant digits are taken, starting at position 4. To enhance even more the important values of this indicator we multiply it by the ratio of the average interval over the 24 most recent seisms (the same range used to calculate μ) over the average interval of the whole series. In this way we obtain a more sensitive indicator which we can call *dilation D*, since it is larger for periods where intervals between seisms increase. We can write

$$D(i,24) = \mu(i,24)b4\_4,3 \times \frac{\langle interval(i) \rangle_{24}}{\langle interval \rangle_{full}} \quad . \tag{2}$$

The previous equation preserves all the features of mutability, but they are amplified by the multiplying function

$$g(i,\nu) = \frac{\langle interval(i) \rangle_{\nu}}{\langle interval \rangle_{full}} \quad , \tag{3}$$

which enhances the behavior of data over the recent interval of ν events. In this way $g(i,\nu)$ is larger than 1.0 when intervals between successive events increase, and is less than 1.0 otherwise; actually it approaches 0.0 when successive events are very frequent, like in the replica regime after important earthquakes.

Fig. 3 shows $g(i,24)$ and $g(i,96)$ for comparison. It shows that the multiplying function $g(i,\nu)$ amplifies the behavior of the mutability $\mu(i,\nu)$, which increases the contrast between periods of high and low occurrence of seisms. Moreover $g(i,\nu)$ tends to be larger for shorter window length ν, which is one of the reasons for picking $\nu = 24$. Of course there is a minimum value of ν to obtain stable results which we found to be around 24 for the present kind of data.

The main body of Fig. 4 presents the results for dilation for the Central Zone series. As it can be seen $D(i,24)$ reaches high values before large earthquakes, while staying at low values for the periods of time where no large quakes were reported in this region or nearby. The inset in Fig. 4 shows $D(i,96)$, where the only change with respect to the main figure is that Eq. (2) is now applied to an interval four times larger than the one in the main figure. As it can be seen the position of the maxima and even relative amplitudes remain about the same. This shows the robustness of the method. We settled for the shortest possible interval (24 events) preserving the same response. In this way we favor an anticipation to events of interest.

There are two major earthquakes involved in Fig. 4. It is interesting to realize that $D(i,24)$ approaches the value 4 about 2800 events (approximately 3 years 8 months) before the earthquake of

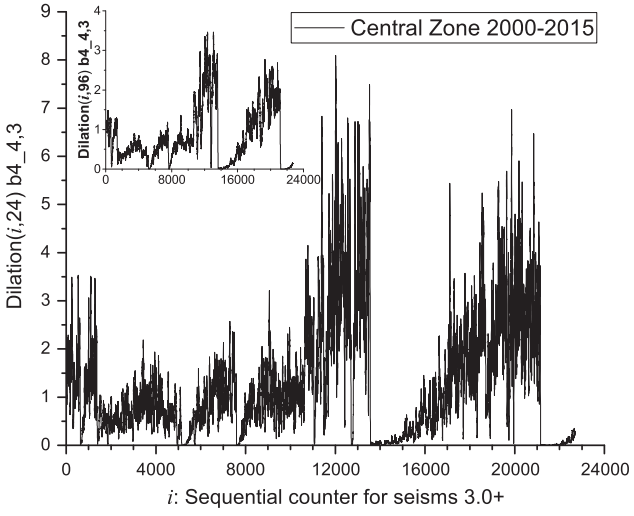

Fig. 4. Dilation $D(i,24)$ for the same data considered in previous figure. It can be noticed that aftershocks are somewhat suppressed, while pre-seismic activity is enhanced. The inset presents $D(i,96)$, namely, a treatment of the same data over a larger interval (see main text for discussion).

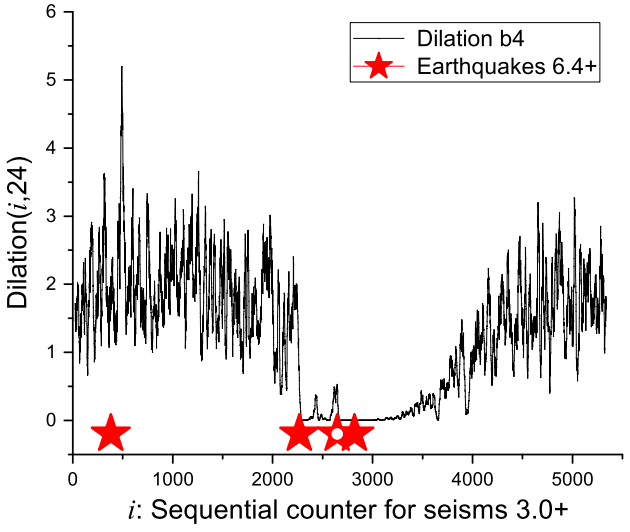

Fig. 5. Dilation $D(i,24)$ for the Iquique data set for seisms of magnitude 3.0 and larger. The presence of the earthquake of April 1, 2014 (magnitude 8.2) is clearly appreciated. Major earthquakes are marked with stars over the abscissa (the hollow star is for the largest earthquake of the series).

2010.02.27, with epicenter in the neighboring Maule region. Then $D(i, 24)$ reaches 4 again about 4000 events (approximately 4 years 6 months) before the earthquake of 2015.09.16.

What is high and what is low depends on the tuning and is probably different for different geographical areas. In spite of this, for the data set studied, it is possible to advert that during the previous few years to a major earthquake the indicator $D(i, \nu)$ increases noticeably with respect to previous values.

We can test this observation for data coming from a different series. For the Iquique region, results for dilation are presented in Fig. 5. The four largest uncorrelated seisms in this area (listed in Table 1 as I1 to I4) are identified with stars over the abscissa axis (the largest one with a hollow star). Similarly to what was observed in Fig. 4, seisms of magnitude below 6.5 do not give an important signal under the tuning used here. However the large seism shows the behavior already discussed in the previous case.

The dilation function is lower for the Iquique data than for the Central Zone data, which has not real meaning. It is only relative values within a region that matters. From Fig. 5 we appreciate that $D(i, 24)$ reached 3.0 about 2300 events (approximately 2 years) before the earthquake of 2014.04.01. Then it reached 3.0 again on 2015.03.23 which could be an indication that an important earthquake could occur in the future in Northern Chile or Southern Peru.

We proceed now to test the robustness of the method with respect to the magnitude thresholds to record data. The data from Iquique is filtered as to retain seisms with magnitude 4.7 and larger only, which leaves a set of 259 seisms. Then, the same procedure outlined in the previous analysis is invoked to obtain the dilation results in quaternary basis with precision 4,3. This function is plotted in Fig. 6. All the features pointed out in the previous paragraph regarding Fig. 5 hold except that now the contrast is larger. This is an indication that the method can be tuned to the level of desired earthquake analysis, and that its capability to anticipate large earthquakes in the studied data is not highly sensitive to the magnitude threshold. Fig. 6 shows that the level of the dilation function is approaching that of the years immediately preceding I3, as also observed for Fig. 5.

Finally, we replicate the very same procedure outlined in the previous paragraph to the set of seisms 4.7+ of the Maule series; results are presented in Fig. 7. As before, the four largest uncorrelated seisms of this series are identified with stars over the abscissa axis (the largest one with a hollow star). It is interesting to notice that the earthquake of 3 March 1985 (M1) produced a short period of

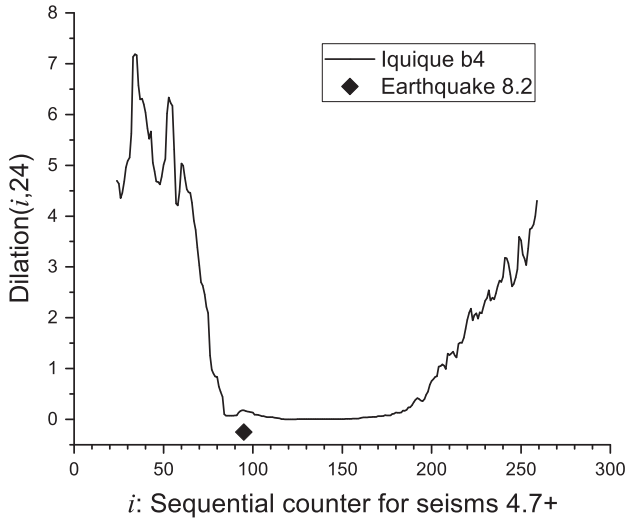

Fig. 6. Dilation $D(i, 24)$ for the Iquique data restricted to seisms of magnitude 4.7 and larger. The time span of this figure is the same one as the one in Fig. 5. A diamond marks the position of the largest earthquake of the series.

frequent aftershock seisms and dilation recovered soon to previous levels. However, after the seism of 27 February 2010 (M2, the sixth largest ever recorded according to the USGS), a longer low dilation behavior is observed. Actually, $D(i, 24)$ remained near 0.0 for three years or so but it is beginning to increase at a much lower rate than the one observed in Fig. 6. Presumably, this can indicate that the next important quake in this area is still in the far future.

Several other works have dealt with the time interval between earthquakes, using various techniques such as establishing the statistical distribution of them during calm periods (Abe and Suzuki, 2005), focusing on the occurrence of major events (Carlson and Res, 1991), or with approaches such as natural time to renormalize the series in the time domain (Varotsos et al., 2005). Of these, the natural time approach is of interest to us, as it has been suggested that it identifies precursory activity to major earthquakes, by means of an

Table 2
Two segments of data for the central zone of Chile. Columns 1 and 4 correspond to the sequential number of seisms 3.0+. Columns 2 and 5 give the intervals in minutes between successive quakes in decimal scale. Columns 3 and 6 give the same number, but in quaternary scale (boldface digits highlight the portion of the record used for information recognition). The first series with short intervals on the left was registered on 22 June 2003, while the second series with long intervals was recorded during several days from 29 November to 6 December 2008.

Short			Large		
i	Decimal	Quaternary	i	Decimal	Quaternary
5264	00032	000**000**200	12653	02403	000**211**203
5265	00028	000**000**130	12654	00282	000**010**122
5266	00007	000**000**013	12655	02502	000**213**012
5267	00002	000**000**002	12656	00995	000**033**203
5268	00035	000**000**203	12657	01639	000**121**213
5269	00015	000**000**033	12658	00332	000**011**030
5270	00028	000**000**130	12659	00362	000**011**222
5271	00011	000**000**023	12660	01425	000**112**101
5272	00026	000**000**122	12661	00656	000**022**100
5273	00014	000**000**032	12662	01228	000**103**030

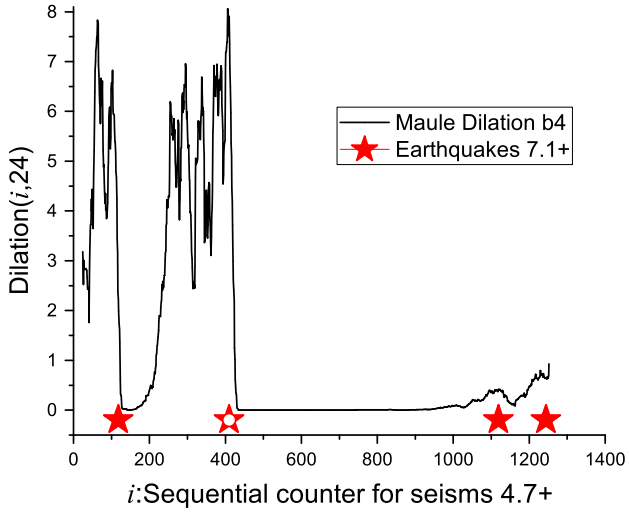

Fig. 7. Dilation $D(i, 24)$ for the Maule data set for seisms 4.7 and stronger. Major earthquakes are marked with stars over the abscissa (hollow star is for largest earthquake of the series).

order parameter taken from the time series of seismic electric signals (SES) or the seismic catalog itself (Sarlis and Christopoulos, 2012; Varotsos et al., 2002, 2011, 2005).

In this work, we are introducing two new and simple parameters to the study of the time interval between seismic events: mutability and dilation. These parameters are extracted from the seismic data, and are thus independent of the availability of concurrent measurements such as seismic electric signals (Varotsos et al., 2006a; Varotsos et al., 2002). On the other hand, our approach seems to exhibit universalities worth studying, such as others found with previous methods like the change in time interval distributions during calm periods (Abe and Suzuki, 2005), or the abrupt decrease/increase of properly defined parameter orders within the natural time approach (Sarlis and Christopoulos, 2012; Varotsos et al., 2005). In our case, we have observed a similar, distinctive behavior of the mutability and the dilation before the three major earthquakes studied.

4. Conclusions

We have shown that information recognition for the series of intervals in the sequence of seisms within a geographical area reveals different regimes in the seismic activity. The use of wlzip allows to tune the recognition to the magnitude of seisms of interest.

When the tuning is focused on the large earthquakes it is found that the dilation, $D(i,24)$, obtained by pattern recognition in quaternary basis, reaches levels higher than average some months before large earthquakes. Although $D(i,24)$ cannot predict exactly when or where an earthquake is going to occur it can be a useful warning to evaluate the seismic risk in active areas.

The analysis done for the Central Zone including seisms 2.0+ (not shown) yielded results similar to those presented in Figs. 2 and 4 only a bit noisier. This encouraged us to filter data bases to seisms of magnitude 4.7+ where major earthquakes stand out in a clearer way as shown by Figs. 6 and 7. At this point we do not want to mean that seisms 4.7+ are the only or right choice to apply the method since each area could have a different dynamics. We just say that by filtering the seismic activity over an appropriate magnitude (which can be tuned for each area), a good contrast for the different regimes can be found.

From the three geographical areas examined here it looks like near Iquique is where energy is accumulating at a larger rate at present. However, it is not possible to venture a possible date for the relaxation of such energy in the form of a major earthquake.

The method presented above can be improved after testing it for data beyond the subduction origin as the dynamics of other processes is probably different. However, the determination of $D(i,\nu)$ offers tunable possibilities which can be adjusted in each case. Actually this has been the case for the application of wlzip to other fields as mentioned in the Introduction. Further research on this approach to seismicity should lead us to a better assessment of its advantages and disadvantages with respect to other methods to evaluate seismic risk.

Several additional studies could also be possible by means of this technique. The analysis of the aftershocks could be done by tuning wlzip in the other direction, namely, to recognize short intervals, closer to what was shown in Fig. 2. A careful study of the failure associated to the subduction of the Nazca plate under the Continental plate could yield information about “hot” spots candidates for future earthquakes. Application to seismic data related to other geographical areas could serve to recognize the universality of this method.

Acknowledgments

One of us (EEV) is grateful to Fondecyt (Chile) under contract 1150019, and Center for the Development of Nanoscience and Nanotechnology (CEDENNA) funded by Conicyt (Chile) under contract FB0807 for partial support. DP thanks Advanced Mining Technology Center (AMTC) and the Fondecyt 11160452. VM thanks Fondecyt project 1161711. We are thankful to Dr. Francisco Muñoz from Universidad de Chile for valuable comments.

References

Abe, S., Pastén, D., Muñoz, V., Suzuki, N., 2011. Chin. Sci. Bull. 56, 3697.
Abe, S., Pastén, D., Suzuki, N., 2010. Physica A 390, 7.
Abe, S., Sarlis, N.V., Skordas, E.S., Tanaka, H.K., Varotsos, P.A., 2005. Phys. Rev. Lett. 94, 170601.
Abe, S., Suzuki, N., 2005. Physica A 350, 588.
Baiesi, M., Paczuski, M., 2004. Phys. Rev. E 69, 066106.
Carlson, J.M., 1991. J. Geophys. Res. B 96, 4255.
Contreras, D.J., Vogel, E.E., Saravia, G., Stockins, B., 2016. J. Am. Soc. Hypertension 10, 217.
Fu, Z., Liu, J., Liu, G., 2004. Tectonophysics 390, 75.
Lonsdale, P., 2005. Tectonophysics 404, 237.
Maksymowicz, A., 2015. Tectonophysics 659, 183.
Manea, V.C., Manea, M., Ferrari, L., Orozco-Esquivel, T., Valenzuela, R.W., Husker, A., Kostoglodov, V., 2017. Tectonophysics 695, 27.
Pastén, D., Comte, D., 2014. J. Seismology 18, 707.
Pastén, D., Muñoz, V., Cisternas, A., Rogan, J., Valdivia, J.A., 2011. Phys. Rev. E 84, 066123.
Pastén, D., Torres, F., Toledo, B., Muñoz, V., Rogan, J., Valdivia, J.A., 2016. Pure Appl. Geophys. 173, 2267.
Romashkova, L.L., 2009. Tectonophysics 470, 329.
Rotondi, R., Varini, E., 2006. Tectonophysics 423, 107.
Sarlis, N.V., Christopoulos, S.R.G., 2012. Chaos 22, 023123.
Sarlis, N.V., Skordas, E.S., Varotsos, P.A., 2009. Phys. Rev. E 80, 022102.
Sarlis, N.V., Skordas, E.S., Varotsos, P.A., 2010. Europhys. Lett. 91, 59001.
Servicio Sismológico Nacional (Chile), 2016. http://ssn.dgf.uchile.cl.
Telesca, L., Cuomo, V., Lapenna, V., Macchiato, M., 2001. Geophys. Res. Lett. 28, 4323.
Telesca, L., Lapenna, V., 2006. Tectonophysics 423, 115.
Telesca, L., Lovallo, M., 2009. Geophys. Res. Lett. 36, 4323.
Telesca, L., Lovallo, M., 2012. Europhys. Lett.. 97. 50002p1.
Telesca, L., Lovallo, M., Lapenna, V., Macchiato, M., 2007. Physica A 377, 279.
United States Geological Survey, 2016. http://www.usgs.gov.
Varotsos, P.A., Sarlis, N.V., Skordas, E.S., 2002. Phys. Rev. E 66, 011902.
Varotsos, P.A., Sarlis, N.V., Skordas, E.S., 2011. Natural time analysis: the new view of time. Precursory Seismic Electric Signals, Earthquakes and Other Complex Time-series. Vol. 1. Springer-Verlag, Berlin, Heidelberg, pp. 19–245.
Varotsos, P.A., Sarlis, N.V., Tanaka, H.K., Skordas, E.S., 2005. Phys. Rev. E 72, 041103.
Varotsos, P.A., Sarlis, N.V., Skordas, E.S., Tanaka, H.K., Lazaridou, M.S., 2006a. Phys. Rev. E 73, 031114.
Varotsos, P.A., Sarlis, N.V., Skordas, E.S., Tanaka, H.K., Lazaridou, M.S., 2006b. Phys. Rev. E 74, 021123.
Vogel, E.E., Saravia, G., 2014. Eur. Phys. J. B 87, 1.
Vogel, E.E., Saravia, G., Astete, J., Díaz, J., Riadi, F., 2015. Physica A 424, 372.
Vogel, E.E., Saravia, G., Bachmann, F., Fierro, B., Fischer, J., 2009. Physica A 388, 4075.
Vogel, E.E., Saravia, G., Cortez, L.V., 2012. Physica A 391, 1591.
Vogel, E.E., Saravia, G., Kobe, S., Schumann, R., Schuster, R., 2016. A Novel Method to Optimize Electricity Generation From Wind Energy. submitted to Renewable Energy.
Xu, Y., Burton, P.W., 2006. Tectonophysics 423, 125.